Combination of Characteristic Green's Function Technique and Rational Function Fitting Method for Computation of Modal Reflectivity at the Optical Waveguide End-facet

Abdorreza Torabi and Amir Ahmad Shishegar
Department of Electrical Engineering, Sharif University of Technology, Tehran, Iran

Keywords: Optical Waveguide End-facet, Guided Mode Reflection Coefficient, Characteristic Green's Function, Complex Images Method, Rational Function Fitting Method, VECTFIT Algorithm, Optimization.

Abstract: A novel method for computation of modal reflectivity at optical waveguide end-facet is presented. The method is based on the characteristic Green's function (CGF) technique. Using separability assumption of the structure and rational function fitting method (RFFM), a closed-form field expression is derived for optical planar waveguide. The uniform derived expression consists of discrete and continuous spectrum contributions which denotes guided and radiation modes effects respectively. An optimization problem is then defined to calculate the exact reflection coefficients at the end-facet for all extracted poles obtained from rational function fitting step. The proposed CGF-RFFM-optimization offers superior exactness in comparison with the previous reported CGF-complex images (CI) technique due to contribution of all components of field in the optimization problem. The main advantage of the proposed method lies in its simple implementation as well as precision for any refractive index contrast. Excellent numerical agreements with rigorous methods are shown in several examples.

1 INTRODUCTION

Optoelectric devices such as laser amplifier, optical modulator and coupler are widely used in integrated optics (IO) circuits. In these applications, facet reflectivity typically deviates the performance of the integrated system from its original designed target. The oldest accepted model for computation of facet reflectivity is Ikegami's model (Ikegami, 1972), which was introduced for double-heterojunction (DH) GaAs-AlGaAs lasers. In this approach, with the use of eigenmode expansion, electric and magnetic fields are matched at the facet. In (Lewin, 1975), an approximate modal reflectivity is developed by means of a plane wave Fresnel reflectivity expansion. Derived expressions are utilized in some other works related to two-dimensional (2-D) buried DH lasers (Hardy, 1984). These results are quite accurate but are just useful for low refractive index contrast. Gelin (Gelin et al., 1981) extended Rozzi's variational treatment (Rozzi and Veld, 1980) for end-facet modal reflectivity and proposed an efficient numerical computation. The main challenge of mode matching based approach is the computation of time-consuming integrals which usually have singular integrands to contribute radiation modes. Moreover, finite window Fourier transform could be combined with perturbation series for fast computation of end-facet reflectivity (Chen et al., 2012).

An efficient way to regard the continuous spectrum contribution in mode matching method is using appropriate set of modes achieved by closing the desired structures with perfectly matched layers (PMLs) (Derudder et al., 2001). The main disadvantage of PML method is the considerable number of discrete modes must be considered to obtain for an appropriate accuracy. A different approach is utilizing iterative based methods. In (Yevick et al., 1991), split-operator method is utilized and the interface of facet is divided into segments in such a way that within each segment the refractive index is nearly constant. The resulting contribution of each segment to the total reflected field is superimposed. Finally a linear iterative equation is obtained which can be solved by classical Neumann series or more stably by bi-conjugate gradient method (Wei and Lu, 2002). In other iterative approach, reflection operator is diagonalized completely or partially (Yevick et al., 1992) using the known eigenmodes and eigenvectors of square root operator. A separate class of solution methods em-

Torabi A. and Shishegar A..
Combination of Characteristic Green's Function Technique and Rational Function Fitting Method for Computation of Modal Reflectivity at the Optical Waveguide End-facet.
DOI: 10.5220/0005332300140021
In *Proceedings of the 3rd International Conference on Photonics, Optics and Laser Technology* (PHOTOPTICS-2015), pages 14-21
ISBN: 978-989-758-093-2

ploy Padé or complex Padé approximations to rational approximation of the square root operator (El-Refaei et al., 2000), (Jamid and Khan, 2007), (Yu and Yevick, 1997). Stability and convergence problem are the main challenges in this approach. For more rigorous solution, integral equation can be used. Parsa and Paknys (Parsa and Paknys, 2007a) used equivalence principle and image theory and model the truncated semi-infinite dielectric slab waveguide by an infinite dielectric slab with unknown current density on a plane just at truncating surface of the end-facet which is solved by the method of moments (MoM). Coupling of the guided modes are incorporated in this method in the form of coupling matrix of end-facet.

In this paper a novel method for computation of guided modes reflectivity at the waveguide end-facet is presented. The proposed method is based on the characteristic Green's function (CGF) technique combined with rational function fitting method (RFFM) (Torabi et al., 2014b), (Torabi et al., 2013). Spatial Green's function of finite dielectric planar waveguide is obtained by separation of the structure into infinite 1-D layered media. For nonseparable structure like typical finite dielectric slab waveguide (i.e. DH laser), using separability assumption, an approximate and closed-form expression for spatial Green's function is achieved. The final formulation is utilized in an efficient optimization problem to find the exact facet reflection coefficients of guided modes. In contrary to previous reported CGF-complex images

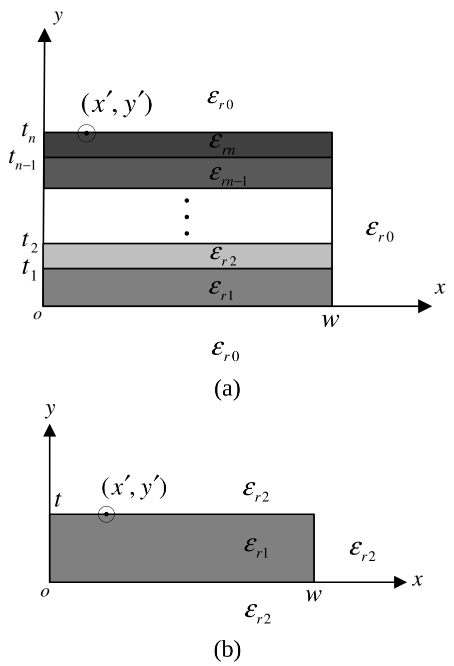

Figure 1: A line source on a truncated (a) multilayered (b) slab waveguide.

(CI) based method (Torabi et al., 2014a), in the formulation of CGF-RFFM continuous spectrum contribution are presented by some poles similar to guided modes part. Then unlike CGF-CI, in CGF-RFFM both discrete and continuous spectrum contributions are efficiently incorporated in the optimization problem. Therefore more exact results of guided modes reflectivity can be obtained. This fact is shown in several examples. Simplicity of implementation as well as precision is the main advantage of the proposed method. Moreover, this method can be used for any planar dielectric waveguides with abrupt termination and also for any refractive index contrasts.

2 CGF-RFFM FORMULATION

2.1 CGF Technique and Separability Assumption

The 2-D Helmholtz's equation should be solved for Green's function of magnetic vector potential, A_z, for a line source surrounded by layered media as it is shown in Fig. 1(a). Here for simplicity the derivations are developed for truncated dielectric slab waveguide shown in Fig. 1(b) for simplicity while the implementation for multilayered media (Fig. 1(a)) is straightforward. The 2-D Helmholtz's equation can be separated into two 1-D equations if (Faraji-Dana, 1993a), (Shishegar and Faraji-Dana, 2003)

$$\varepsilon_r(x,y) = \varepsilon_x(x) + \varepsilon_y(y). \tag{1}$$

By the assumption of (1), the original structure has been decomposed into two layered media denoted by N_x and N_y layered media (Fig. 2(a) and Fig. 2(b), N_γ called *normal to* γ where $\gamma = x, y$), which their relative dielectric constants are $\varepsilon_x(x)$ and $\varepsilon_y(y)$ respectively. If this separation is rigorously possible, it means that the original structure, Fig. 1(b), can be exactly reproduced by crossing two 1-D N_x and N_y layered media which is shown in Fig. 2(c). The solutions to the 1-D Helmholtz's equations are denoted by G_x (for Fig. 2(a)) and G_y (for Fig. 2(b)) and can be obtained analytically using usual spectral techniques (Michalski and Mosig, 1997). We will have,

$$G_\gamma(\gamma,\gamma') = \frac{(1+R_\gamma e^{-j2\beta_{\gamma1}\gamma_<})(1+R_\gamma e^{-j2\beta_{\gamma1}(d_\gamma-\gamma_>)})e^{-j\beta_{\gamma1}(\gamma_>-\gamma_<)}}{(2j\beta_{\gamma1})(1-R_\gamma^2 e^{-j2\beta_{\gamma1}d_\gamma})}, \tag{2}$$

$$R_\gamma = \frac{\beta_{\gamma1}-\beta_{\gamma2}}{\beta_{\gamma1}+\beta_{\gamma2}}, \tag{3}$$

where d_γ is equal to w and t for $\gamma = x$ and y respectively. $\gamma_>$ and $\gamma_<$ are greater and smaller values of γ and γ' respectively and $\beta_{\gamma i} = \sqrt{\varepsilon_{\gamma i} k_0^2 + \lambda_\gamma} \quad (i = 1,2)$. R_x and R_y are the reflection coefficients of a TE wave at the interfaces (due to the symmetry $R_{Ax} = R_{Bx} = R_x$ and $R_{Ay} = R_{By} = R_y$ in Fig. 2). Then having G_x and G_y, the solution of A_z for separable structure of Fig. 2(c) is given by (Faraji-Dana, 1993a), (Shishegar and Faraji-Dana, 2003)

$$A_z(x,y;x',y') = \left(\frac{-1}{2\pi j}\right) \oint_{C_{\lambda y}} G_x(x,x',-\lambda_y) G_y(y,y',\lambda_y) d\lambda_y, \qquad (4)$$

where the contour $C_{\lambda y}$, encloses only the singularities of G_y, (including branch cut, branch point and discrete poles singularities), in counterclockwise sense. For the structure at hand, Fig. 1(b), it can be shown that the separation of (1), is not rigorously possible (Shishegar and Faraji-Dana, 2003). If one ignore (1) in four exterior regions in Fig. 2(c), then an infinite number of solutions for ε_{x1}, ε_{x2}, ε_{y1} and ε_{y2} could be found. It must be noted that the solutions are not physically available relative dielectric constants. They are just mathematical quantities. One can choose $\varepsilon_{x1} = 0$, $\varepsilon_{x2} = \varepsilon_{r2} - \varepsilon_{r1}$, $\varepsilon_{y1} = \varepsilon_{r1}$, $\varepsilon_{y2} = \varepsilon_{r2}$ for N_x and N_y media. For all possible solutions, the corner regions of the original structure are replaced by $\varepsilon_{x2} + \varepsilon_{y2} = 2\varepsilon_{r1} - \varepsilon_{r2}$ (Shishegar and Faraji-Dana, 2003). This deviation makes the CGF result in (4) an approximate Green's function for original structure (Fig. 1(b)). It should be noted that for multilayered truncated waveguide (with n layers) of Fig. 1(a), after separation, the N_y layered media would be a 1-D infinite layered media (with n layers) while N_x media would be the same as Fig. 2(a). So it is just sufficient that G_y of related N_y layered media is computed analytically and incorporated in integral representation of (4).

2.2 CGF-RFFM

In common optical waveguide structures, t is much smaller than w. So, with acceptable approximation, guided modes (surface wave poles) of CGF G_y (Fig. 2(b)) denote the guided modes of the original structure in Fig. 1(b). Furthermore, the integration of (4) in CGF technique is so time consuming and expensive due to highly oscillatory nature of its integrand. To circumvent the numerical integration of (4), rational function fitting method can be used. In CGF-RFFM the G_y is first approximated by appropriate set of discrete poles via modified VECTFIT algorithm (Torabi et al., 2014b). Like,

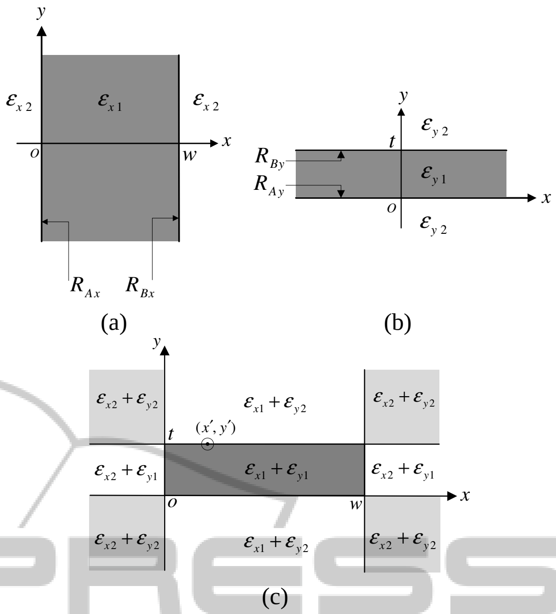

Figure 2: (a) N_x and (b) N_y layered media, (c) Separable structure analyzed instead of original structure in CGF technique.

$$G_y(y,y',\lambda_y) \approx \sum_{m=1}^{N_p} \frac{\mathrm{Res}_m}{\lambda_y - \lambda_{ym}} \qquad (5)$$

where Res_m is the residue of G_y at the mth pole. N_p is the number of poles used in RFFM for rational fitting. It should be noted that the set of extracted poles in (5) includes guided modes of the structure. Moreover, some other poles are also extracted that are responsible to construct the continuous spectrum contribution. Therefore, these poles have similar characteristic to leaky wave poles and so we may call them quasi leaky wave poles (Torabi et al., 2014b). Then by substituting (5) in (4) and applying residue theorem, a closed form series representation for A_z will be obtained and can be found by (6). In (6), $k_{xm} = \sqrt{\varepsilon_{x1} k_0^2 - \lambda_{ym}}$ is the propagation constant of the mth mode in the x-direction. Since the rational function fitting of (5) would have excellent accuracy, therefore a closed form relation of (6) can approximate the integral of (4) very well. We can separate A_z of (6) in two terms like (7) where A_z^g denotes the guided modes part (or discrete spectrum contribution) and is in series form of (6) in which just guided modes (surface wave poles) contributes while A_z^r related to radiation modes part (or continuous spectrum contribution) and is in series form of (6) in which the non surface wave poles (quasi leaky wave poles) contributes.

In (6), R_{xm} is the reflection coefficient of modes

$$A_z = \sum_{m=1}^{N_p} -\mathrm{Res}_m \frac{(1+R_{xm}e^{-j2k_{xm}x_<})(1+R_{xm}e^{-j2k_{xm}(w-x_>)})e^{-jk_{xm}(x_>-x_<)}}{(2jk_{xm})(1-R_{xm}^2 e^{-j2k_{xm}w})}, \tag{6}$$

$$\begin{aligned} A_z &= A_z^g + A_z^r, \\ A_z^g &= \sum_{m=1}^{N_{\mathrm{guided}}} -\mathrm{Res}_m \frac{(1+R_{xm}e^{-j2k_{xm}x_<})(1+R_{xm}e^{-j2k_{xm}(w-x_>)})e^{-jk_{xm}(x_>-x_<)}}{(2jk_{xm})(1-R_{xm}^2 e^{-j2k_{xm}w})}, \\ A_z^r &= \sum_{m=1}^{N_p-N_{\mathrm{guided}}} -\mathrm{Res}_m \frac{(1+R_{xm}e^{-j2k_{xm}x_<})(1+R_{xm}e^{-j2k_{xm}(w-x_>)})e^{-jk_{xm}(x_>-x_<)}}{(2jk_{xm})(1-R_{xm}^2 e^{-j2k_{xm}w})}, \end{aligned} \tag{7}$$

at the N_x interface shown in Fig. 3(a). But actually, these modes are reflected from truncated surface of the substrate shown in Fig. 3(b). This discrepancy arises from the separability approximation of the original structure which also makes the refractive index of four exterior corners deviate from its exact value. For low refractive index contrast, $\varepsilon_{r1} \approx \varepsilon_{r2}$, as is common in optical buried waveguides, the error in A_z due to approximate modeling of the corner regions is ignorable because $2\varepsilon_{r2} - \varepsilon_{r1} \approx \varepsilon_{r2}$. But in high refractive index contrasts, considerable deviation may be imposed on the Green's function especially for source and field points close to the corners. Therefore to have exact A_z for truncated dielectric slab waveguide of Fig. 1(b) both terms A_z^g and A_z^r should be corrected. Although having enough distance from corners for source and field point makes the deviation in A_z^r part small but for more accurate results of reflection coefficients of guided modes, correction of A_z^r part along with A_z^g part should be considered. Before defining the optimization problem, it should be noted that the main difference between proposed CGF-RFFM and CGF-CI method (Torabi et al., 2014a) is in the approximation form of G_y. In CGF-CI the surface wave poles are first extracted from G_y in a similar form of (5) and the remaining part is approximated exponentially by GPOF approach (Hua and Sarkar, 1989). In fact by CGF-RFFM, unlike CGF-CI, a uniform representation of G_y as well as A_z can be achieved and it will be shown that it leads to more accurate results of reflection coefficients.

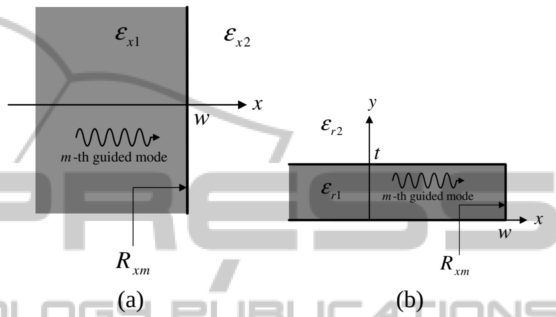

Figure 3: Reflection of mth SW at the (a) interface of N_x structure, and (b) end-facet.

3 OPTIMIZATION PROBLEM

Exact values of A_z for field points (x_i, y_i), $i = 1,2,\ldots,N_f$ can be achieved by CAD tools like COMSOL which is fast and accurate and are capable of solving 2-D problem like Fig. 1. Moreover, exterior-interior method of moments (MoM) can be used for problem of Fig. 1 to find exact A_z (Faraji-Dana, 1993b). Consider the field distribution on the upper surface of the waveguide, $y = t$, in Fig. 1(b). The line source is located at $x' = w/2$ and $y' = t$. Suppose that the exact result of A_z is denoted by A_z^{exact}. If we consider R_{xm}, $m = 1,2,\ldots,N_p$ in (6) as unknowns, then a following optimization problem can be defined for computation of the exact R_{xm} at the end-facets of truncated slab shown in Fig. 1

$$\min_{\substack{R_{xm},\\ m=1,2,\ldots,N_p.}} \quad f_{\mathrm{error}}(R_{x1}, R_{x2}, \ldots, R_{xN_p}), \tag{8}$$

$$f_{\mathrm{error}} = \sum_{i=1}^{N_f} \left| A_z(x_i, y_i; x', y'; R_{x1}, R_{x2}, \ldots, R_{xN_p}) - A_z^{exact}(x_i, y_i; x', y') \right|^2. \tag{9}$$

To solve the optimization problem, subspace trust-region algorithm is used which is based on the interior-reflective Newton method described in (Coleman and Li, 1996). By increasing the number of field points, N_f, more exact R_{xm}s will be obtained. For initial values of R_{xm}s, one can use $\frac{\beta_{x1}-\beta_{x2}}{\beta_{x1}+\beta_{x2}}\Big|_{\lambda_y=\lambda_{ym}}$ for R_{xm}, obtained in CGF method (3). More rapid convergence and rigorous results can be obtained by using modified initial values of R_{xm} such as Marcateli's approximation $R_{xm} = \frac{n_m - n_2}{n_m + n_2}$ where $n_2 = \sqrt{\varepsilon_{r2}}$ and the effective index n_m is calculated from the propagation constant of N_y guided mode. i.e. $n_m = \frac{k_{xm}}{k_0}$. More accurate closed-form expression for R_{xm} can be found

Table 1: R_{x1} for low and high refractive index contrast structure shown in Fig. 1(b) with $w = 2\lambda$, for $N_f = 200$ observation points using CGF-RFFM-optimization, CGF-CI-optimization with $d_s = w/10$, and mode matching methods (Gelin et al., 1981). Mean time for computation of A_z^{exact} by COMSOL is less than 8sec.

	$\frac{t}{\lambda}$	n_1	n_2	CGF-RFFM-optimization	CGF-CI-optimization	(Gelin et al., 1981)
Structure 1	0.1	1.46	1.45	-0.760+j0.038	-0.735+j0.088	-0.761+j0.039
Structure 2	0.1	2.6	2.5	-0.468-j0.372	-0.472-j0.379	-0.468-j0.372
Structure 3	0.1	4.472	1	0.688+j0.232	0.672+j0.228	0.688+j0.231
Structure 4	0.166	4.472	1	0.716+j0.151	0.711+j0.142	0.718+j0.155
Structure 5	0.08	5.477	1	0.651+j0.396	0.649+j0.391	0.651+j0.399
Mean time				$<$ 5 sec	$<$ 2 sec	$>$ 8 min

in (Lewin, 1975).

The main advantage of using CGF-RFFM is that all extracted poles can incorporate in the optimization problem of (8). While in CGF-CI method (Torabi et al., 2014a) the part of continuous spectrum contribution (A_z^{CS} in (Torabi et al., 2013)) which is related to approximate separable structure of Fig. 2(c) is first subtracted by exact A_z and the remained part is used to optimized discrete spectrum contribution to find R_{xm} of guided modes. Therefore in (9) both discrete and continuous spectrum parts would be corrected by optimizing all the R_{xm} of extracted poles including guided and quazi-leaky wave poles. This is in fact due to the capability of the rational function fitting method to obtain uniform expansion of A_z in (5). So it is expected that more accurate R_{xm} of guide modes could be found by CGF-RFFM than CGF-CI method. Although the time of optimization process would be increased due to more poles incorporated in (9) but results of next section shows that this is ignorable in comparison with the gained accuracy.

4 NUMERICAL RESULTS

To show the efficiency and versatility of the proposed approach rigorous methods such as mode matching is utilized (Gelin et al., 1981). More, CGF-CI-optimization (Torabi et al., 2014a) results are also provided. RFFM step which includes poles extraction from G_y can be so fast. Then, to have exact reflection coefficients, optimization step should be run for N_f sample field points in $[0, w]$ where the exact A_z are available there. We place the source far from the corners to have more exact results from CGF-RFFM in (6). More it should be noted here that in CGF-CI based method a guard d_s is considered and the samples are chosen in $[d_s, w - d_s]$. This is due to the fact that contribution of continuous spectrum of separable structure, Fig. 2(c), largely deviates from its original value for nonseparable structure, Fig. 1(b), especially near the corners. But in CGF-RFFM there is no need for any guard because continuous spectrum contribution is also incorporated and corrected in the optimization process along with discrete spectrum contribution. It should be noted that Green's function A_z includes only TE guided modes of the Fig. 1(b). Therefore by using and incorporating A_z in defined optimization problem, reflection coefficients of TE guided modes can be obtained. To have results for TM guided modes one can easily use Green's function of scalar or vector electric potential and follow the similar steps.

At first, let us consider low refractive index contrasts. Results for reflection coefficient of guided mode for structure 1 and 2 with parameters ($n_1 = 1.46$, $n_2 = 1.45$, $t = 0.1\lambda$) and ($n_1 = 2.6$, $n_2 = 2.5$, $t = 0.1\lambda$) respectively, are shown in Table 1. Simulation results for higher refractive index contrast are also reported in Table 1 for structures 3, 4, 5 which have single guided mode. We can find excellent agreement between proposed method and rigorous mode matching method (Gelin et al., 1981). For single guided mode supported waveguide considered in Table 1, mean simulation time for optimization is less than 4 sec. Disregarding the time for preprocessing of the structure to find the exact A_z, our method is much faster than mode matching method. Furthermore, by adding required time of step 1 (which is approximately 8 sec in COMSOL for high accuracy), total CPU-time would still be less than mode matching method. moreover, it can be seen from Table 1 that CGF-RFFM leads to more accurate results in comparison with CGF-CI results. For rational function fitting step of (5), $N_p = 14$ poles are used in modified VECTFIT algorithm.

The number of observation points N_f may be an important parameter in controlling the speed and accuracy of the method. In Table 2, amplitude of optimized R_{xm} for two of considered structures in Table 1 can be found for different N_f. Small changes in optimized reflection coefficient can be seen, by increasing

Table 4: Reflection coefficients for structure shown in Fig. 4 with $n_1 = 1.132$, $n_2 = 2.449$, $n_3 = 3.162$, $n_0 = 1$, $t_1 = 0.1\lambda$, $t_2 = 0.2\lambda$, $t_3 = 0.4\lambda$, $w = 2\lambda$, for $N_f = 200$ observation points using CGF-RFFM-optimization, CGF-CI-optimization (Torabi et al., 2014a) with $d_s = w/10$, and mode matching methods (Gelin et al., 1981). Mean time for computation of A_z^{exact} by COMSOL is less than 8sec.

R_{xm}	CGF-RFFM-optimization	CGF-CI-optimization	(Gelin et al., 1981)
R_{x1}	0.295+j0.717	0.286+j0.722	0.293+j0.716
R_{x2}	0.753+j0.107	0.721+j0.085	0.755+j0.109
Time	$<$ 10 sec	$<$ 5 sec	$>$ 10 min

Table 2: Amplitude of optimized R_{x1} for structure 4 and 5 for different number of observation points N_f

N_f	Structure 4 $\lvert R_{x1}\rvert$	Structure 5 $\lvert R_{x1}\rvert$
150	0.723	0.759
200	0.726	0.762
250	0.728	0.764
300	0.728	0.765

N_f. It can be concluded that with small N_f, quite exact reflection coefficient with high speed can be obtained. In Table 3, Reflection coefficients for a structure with parameter ($n_1 = 5.477$, $n_2 = 1$, $t = 0.19\lambda$) that has three guided TE modes are reported. Excellent match between the results of CGF-RFFM-optimization and IE-MoM can be found (Parsa and Paknys, 2007b). Required simulation time for optimization is near to 8 sec which is much less than exact IE-MoM based method.

To search the versatility of the proposed method let us consider a problem of modal reflectivity at end-facet of of three-layer media of Fig. 4. The refractive indices of layers are $n_1 = 1.132$, $n_2 = 2.449$, $n_3 = 3.162$, $n_0 = 1$, with thickness of $t_1 = 0.1\lambda$, $t_2 = 0.2\lambda$, $t_3 = 0.4\lambda$ that leads to two supporting guided modes. Results for reflection coefficient of guided modes obtained by CGF-RFFM-optimization are reported in Table 4 along with the results of CGF-CI-optimization and mode matching method are also given. $N_p = 16$ poles are considered for rational function fitting step of (5). In comparison with CGF-CI-optimization results excellent match between CGF-RFFM results and exact mode matching method (Gelin et al., 1981) is evident. Moreover, from Table 1 and Table 2, increasing in simulation time of CGF-RFFM due to incorporation of more poles in optimization step is ignorable.

The number of observation points N_f has marginal effects on the speed and accuracy of the method. In Fig. 5(a) and Fig. 5(b) magnitude and phase of the optimized R_{x1} and R_{x2} for structure of Fig. 4 (described

Table 3: Reflection coefficients for structure shown in Fig. 1 with $n_1 = 5.477$, $n_2 = 1$, $t = 0.19\lambda$, $w = 2\lambda$, $N_f = 200$.

R_{xm}	CGF-RFFM -optimization	IE-MoM (Parsa and Paknys, 2007b)
R_{x1}	-0.263+j0.654	-0.263+j0.752
R_{x2}	0.443+j0.758	0.443+j0.759
R_{x3}	0.315+j0.841	0.315+j.841
Time	$<$ 8 sec	$>$ 6 min

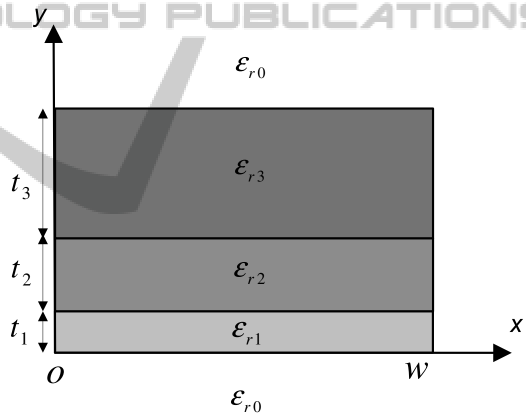

Figure 4: Three layer truncated dielectric slab waveguide.

in Table 4) are depicted for N_f. Good convergence can be seen in the optimized reflection coefficients, by increasing N_f.

5 CONCLUSION

A novel method for reflection of guided mode at the end-facet of optical waveguide is presented. The method is based on the formulation of characteristics Green's function which is combined with rational function fitting method. In the closed-form derivation for spatial Green's function of finite dielectric slab waveguide, discrete and continuous spectrum contribution are expressed in appropriate forms which can be imported in optimization problem to obtain an exact reflection coefficients of guided modes. The main

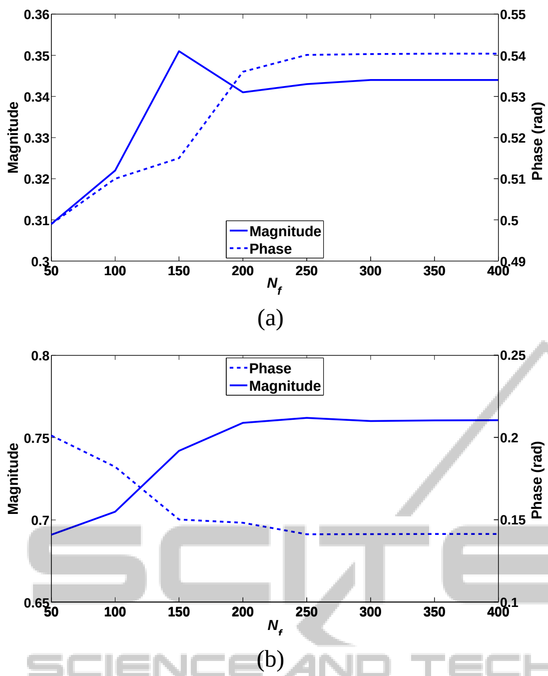

Figure 5: Convergence of magnitude and phase of optimized a) R_{x1} and b) R_{x2}, for different N_f for structure of Table 4.

advantages of this method lie in its rapidity as well as accuracy. By using COMSOL for exact results of spatial Green's function for optimization, total CPU-time is much less than rigorous methods. In general, for all planar multilayered waveguide the formulation can be easily derived for all components of dyadic Green's function to have reflection coefficients of guided modes at the end-facet of truncation.

REFERENCES

Chen, Y., Lai, Y., Chong, T. C., and Ho, S.-T. (2012). Exact solution of facet reflections for guided modes in high-refractive-index-contrast sub-wavelength waveguide via a fourier analysis and perturbative series summation: Derivation and applications. *J. Lightw. Technol.*, 30(15):2455–2471.

Coleman, T. F. and Li, Y. (1996). An interior trust region approach for nonlinear minimization subject to bounds. *SIAM journal on optimization*, 6(2):418–445.

Derudder, H., Olyslager, F., De Zutter, D., and van den Berghe, S. (2001). Efficient mode-matching analysis of discontinuities in finite planar substrates using perfectly matched layers. *IEEE Trans. Antennas Propag.*, 49(2):185 –195.

El-Refaei, H., Betty, I., and Yevick, D. (2000). The application of complex Pade approximants to reflection at optical waveguide facets. *IEEE Photon. Technol. Lett.*, 12(2):158–160.

Faraji-Dana, R. (1993a). *An Efficient and Accurate Green's Function Analysis of Packaged Microwave Integrated Circuits*. Thesis (Ph.D.)–University of Waterloo.

Faraji-Dana, R. (1993b). *An Efficient and Accurate Green's Function Analysis of Packaged Microwave Integrated Circuits*. Thesis (Ph.D.)–University of Waterloo.

Gelin, P., Petenzi, M., and Citerne, J. (1981). Rigorous analysis of the scattering of surface waves in an abruptly ended slab dielectric waveguide. *IEEE Trans. Microw. Theory Techn.*, 29(2):107 – 114.

Hardy, A. (1984). Formulation of two-dimensional reflectivity calculations for transverse-magnetic-like modes. *J. Opt. Soc. Am. A.*, 1(7):760–763.

Hua, Y. and Sarkar, T. (1989). Generalized pencil-of-function method for extracting poles of an EM system from its transient response. *IEEE Trans. Antennas Propag.*, 37(2):229 –234.

Ikegami, T. (1972). Reflectivity of mode at facet and oscillation mode in double-heterostructure injection lasers. *IEEE J. Quantum Electron.*, 8(6):470–476.

Jamid, H. and Khan, M. (2007). 3-D full-vectorial analysis of strong optical waveguide discontinuities using Pade approximants. *IEEE J. Quantum Electron.*, 43(4):343–349.

Lewin, L. (1975). A method for the calculation of the radiation-pattern and mode-conversion properties of a solid-state heterojunction laser. *IEEE Trans. Microw. Theory Techn.*, 23(7):576–585.

Michalski, K. and Mosig, J. (1997). Multilayered media Green's functions in integral equation formulations. *IEEE Trans. Antennas Propagat.*, 45(3):508 –519.

Parsa, A. and Paknys, R. (2007a). Interior Green's function solution for a thick and finite dielectric slab. *IEEE Trans. Antennas Propag.*, 55(12):3504 –3514.

Parsa, A. and Paknys, R. (2007b). Interior Green's function solution for a thick and finite dielectric slab. *IEEE Trans. Antennas Propag.*, 55(12):3504 –3514.

Rozzi, T. and Veld, G. (1980). Variational treatment of the diffraction at the facet of d.h. lasers and of dielectric millimeter wave antennas. *IEEE Trans. Microw. Theory Techn.*, 28(2):61–73.

Shishegar, A. A. and Faraji-Dana, R. (2003). A closed-form spatial Green's function for finite dielectric structures. *Electromagnetics*, 23(7):579–594.

Torabi, A., Shishegar, A. A., and Faraji-Dana, R. (2013). Application of the characteristic Green's function technique in closed-form derivation of spatial Green's function of finite dielectric structures. In *Computational Electromagnetics Workshop (CEM), 2013*, pages 54–55.

Torabi, A., Shishegar, A. A., and Faraji-Dana, R. (2014a). Analysis of modal reflectivity of optical waveguide end-facets by the characteristic Green's function technique. *J. Lightw. Technol.*, 32(6):1168–1176.

Torabi, A., Shishegar, A. A., and Faraji-Dana, R. (2014b). An efficient closed-form derivation of spatial Green's function for finite dielectric structures using characteristic Green's function-rational function fitting method. *IEEE Trans. Antennas Propagat.*, 62(3).

Wei, S. H. and Lu, Y. Y. (2002). Application of Bi-CGSTAB to waveguide discontinuity problems. *IEEE Photon. Technol. Lett.*, 14(5):645–647.

Yevick, D., Bardyszewski, W., Hermansson, B., and Glasner, M. (1991). Split-operator electric field reflection techniques. *IEEE Photon. Technol. Lett.*, 3(6):527–529.

Yevick, D., Bardyszewski, W., Hermansson, B., and Glasner, M. (1992). Lanczos reduction techniques for electric field reflection. *J. Lightw. Technol.*, 10(9):1234–1237.

Yu, C. and Yevick, D. (1997). Application of the bidirectional parabolic equation method to optical waveguide facets. *J. Opt. Soc. Am. A.*, 14(7):1448–1450.